

# Iron line profiles including emission from within the innermost stable orbit of a black hole accretion disc

A.J. Young<sup>1</sup>, R.R. Ross<sup>1,2</sup> and A.C. Fabian<sup>1</sup>

<sup>1</sup>*Institute of Astronomy, Madingley Road, Cambridge CB3 0HA*

<sup>2</sup>*Department of Physics, College of the Holy Cross, Worcester, MA*

27 July 2021

## ABSTRACT

Reynolds & Begelman (1997) have recently proposed a model in which the broad and extremely redshifted iron line seen during a deep minimum of the light curve of the Seyfert 1 galaxy MCG–6–30–15 originates from matter spiralling into a Schwarzschild black hole, contrary to previous claims that the black hole may be spinning rapidly (Iwasawa et al 1996; Dabrowski et al 1997). Here we calculate in detail the X-ray spectrum produced by their model using the full reflected continuum emission, including absorption features. This calculation takes into account the doppler and relativistic effects. For the range of parameters we consider, we find that the spectrum should show a large photoelectric absorption edge of iron, which is not seen in the data. The absorption edge is a consequence of the line emitting matter within the innermost stable orbit being highly ionized, and is largely independent of the parameters chosen for their model. If we restrict our attention to the 3–10 keV band we may effectively remove this absorption edge by fitting a steeper power law, but this results in a significant underprediction of the 0.4–0.5 keV flux. We conclude that the data on MCG–6–30–15 are more consistent with the Kerr than the Schwarzschild model.

**Key words:** accretion discs – black hole physics – galaxies: individual: MCG–6–30–15 – line: profiles – X-rays: general

## 1 INTRODUCTION

Iwasawa et al (1996) have found tentative evidence that the black hole in the Seyfert 1 galaxy MCG–6–30–15 is spinning rapidly. The iron  $K\alpha$  emission line in that source (Tanaka et al 1995) was seen to shift to lower energies during a deep minimum of the light curve, and to have an extremely large equivalent width  $\sim 1$  keV. The iron line emission is thought to originate from fluorescence in the accreting matter, and the photons reaching a distant observer are doppler and transverse-doppler shifted due to the motion of the matter, and gravitationally redshifted in escaping the deep potential well of the black hole. In the case of an accretion disc around a Schwarzschild black hole stable circular orbits can only exist beyond the radius of marginal stability,  $r_{ms} = 6m = 6GM/c^2$ . The observations require a greater redshift than can be explained by fluorescence from matter in a disc extending in to this radius. A disc around a spinning Kerr black hole, however, can extend further in to regions where the gravitational redshift is stronger. Such a disc can provide the necessary additional redshifted flux. A study by Dabrowski et al (1997) has shown that, if this is the case, then the data require that the specific angular momentum of the black hole exceeds 0.95.

Recently Reynolds & Begelman (1997) have proposed

an alternative model, hereafter RB97, in which the necessary additional redshifted flux is provided by fluorescence in optically-thick ionized matter spiralling in from the innermost stable orbit around a Schwarzschild black hole. If this can provide a satisfactory fit to the data then any conclusions on black hole spin made from present X-ray iron line profiles are ambiguous. As they note, a rapidly spinning black hole in a radio-quiet AGN (such as that implied by the maximal Kerr result for MCG–6–30–15) is contrary to some schemes for explaining radio loudness (e.g. Rees et al 1982; Wilson & Colbert 1995).

In the RB97 model the accretion disc is assumed to extend in to the radius of marginal stability,  $6m$ , within which matter is freely falling into the black hole. The matter free-falling within  $6m$  does not dissipate any gravitational potential energy, and is unable to support its own corona. To produce fluorescence in this matter it needs to be illuminated by some external X-ray source, which is approximated by a point source along the rotation axis of the disc. As the material falls from  $6m$  its density drops rapidly and it becomes highly ionized as it approaches the black hole. The fluorescent line that the illuminated matter produces is very dependent upon its ionization state and a useful quantity is the ionization parameter  $\xi(r) = 4\pi F_x(r)/n(r)$ , where  $F_x(r)$  is the X-ray flux received per unit area of the disc at a ra-

dius  $r$ , and  $n(r)$  is the comoving electron number density. The iron line emission for various ionization parameters has been investigated by Matt et al (1993, 1996) and they conclude the following for various values of  $\xi$ .

1.  $\xi < 100 \text{ ergs cm s}^{-1}$  the material produces a ‘cold’ iron line at 6.4 keV and only a small absorption edge.
2.  $100 \text{ ergs cm s}^{-1} < \xi < 500 \text{ ergs cm s}^{-1}$  does not produce an iron line because photons near the line energy are resonantly trapped and lost due to Auger ejections. There is a moderate absorption edge.
3.  $500 \text{ ergs cm s}^{-1} < \xi < 5000 \text{ ergs cm s}^{-1}$  produces a ‘hot’ iron line at 6.8 keV with twice the fluorescent yield of the cold line. There is a large absorption edge.
4.  $\xi > 5000 \text{ ergs cm s}^{-1}$  does not produce an iron line because the iron is completely ionized. There is no absorption edge.

As the matter falls toward the black hole its ionization parameter increases monotonically, so there will be four regions within  $6m$ , each identified with one of the ranges of ionization parameter given above. Fig. 1 shows the typical behaviour of  $\xi$ , for the RB97 model, within  $6m$ . The first region just within  $6m$  is very small since the ionization parameter quickly exceeds  $100 \text{ ergs cm s}^{-1}$ , and there will be an annulus of material further in that may produce a hot line. It is the emission from this region that provides the highly redshifted flux that is required to fit the data. The reflected continuum produced in this region necessarily has an absorption edge associated with it, and it is important to consider the effect of this on the predicted spectrum. In computing the line profile they expect from their model Reynolds & Begelman (1997) treat the iron emission line as a delta function in the rest frame of the gas, which is then broadened by doppler and relativistic effects. Here we use the entire reflected X-ray spectrum, including the absorption edge, which will also be smeared by the doppler and relativistic effects. One may expect the absorption edge to be observable, and that, since the edge will also be highly redshifted, some of the line flux may fall into the edge. Here we compute in detail the expected spectrum from the RB97 model. It is important to do this because there is no clear evidence for absorption in the MCG–6–30–15 data, and there is the possibility that the smeared absorption edge may affect the observed line profile.

## 2 REST FRAME REFLECTION SPECTRA

The two main parameters in the RB97 model, namely the height of the point source above the disc  $h$ , and the overall radiative efficiency of the accretion disc  $\eta_x$ , have to be finely tuned in order to produce a line profile that agrees qualitatively with the data. We adopt parameters typical of those determined by RB97 in which the X-ray continuum, a power law of photon index 2, is assumed to originate at a height  $h = 3.5m$  along the rotation axis of the disc. A small proportion of these photons will reach a distant observer, but many will be bent towards to disc and blueshifted, causing an enhancement in the illuminating intensity seen by the accreting matter. We have calculated this numerically to determine the ionization parameter as a function of radius. Reynolds & Begelman (1997) note that the ionization

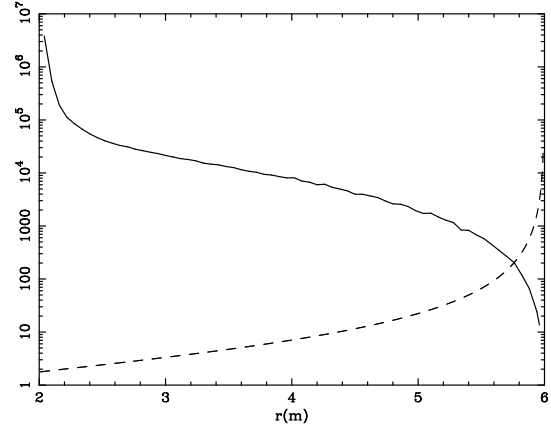


**Figure 1.** Ionization parameter  $\xi$  (solid line) and optical depth  $\tau_e$  as functions of radius for a source height  $h = 3.5m$  and efficiency  $\eta_x = 0.003$ .

state is independent of the mass accretion rate and accretion disc viscosity law since the velocity is approximated by the local free-fall value and the continuum luminosity is a fixed fraction  $\eta_x$  of the total accretion power extractable from a Schwarzschild black hole. The density of the infalling matter follows their expression (18). In Fig. 1 we plot the ionization parameter and the Thomson depth through the infalling matter as functions of radius. Although we have not explored the entire parameter space, choosing different values for these parameters should not qualitatively alter our results since, in order to fit the data, there must be an annulus of emitting material significantly within  $6m$  and this must also have an associated absorption edge. There is little freedom in the choice of parameters  $h$  and  $\eta_x$  if the RB97 model is to produce a line similar to that seen in the data.

The reflected X-ray continuum is computed in a frame in which the gas is at rest. At a given radius the illuminating flux seen by the matter in its rest frame and the ionization parameter are known, and we use the method of Ross & Fabian (1993) to compute the reflected spectrum. This calculation takes into account the vertical ionization structure, Compton scattering and resonant absorption within the matter. The energy resolution is variable, with the greatest resolution near the emission line features, and is significantly higher than the broad line and edge features we wish to discuss later. We have computed spectra for both solar and twice solar iron abundances, and beyond  $6m$  we have assumed the disc to be cold. The spectra were calculated at 11 different radii, and we linearly interpolate between them to obtain the spectrum at a particular radius. Fig. 2 shows the results of these calculations at a number of radii for solar iron abundance. The ionization parameter increases with decreasing radius and the four regions discussed above are illustrated. Other spectral features can be seen below 6 keV, and are due to the fluorescent lines of other metals.

## 3 THE OBSERVED SPECTRUM

To compute the predicted spectrum from the RB97 model we trace photon paths backwards from a hypothetical observer through an array of equal solid angle pixels until they hit the accretion disc or enter the black hole. The observer is

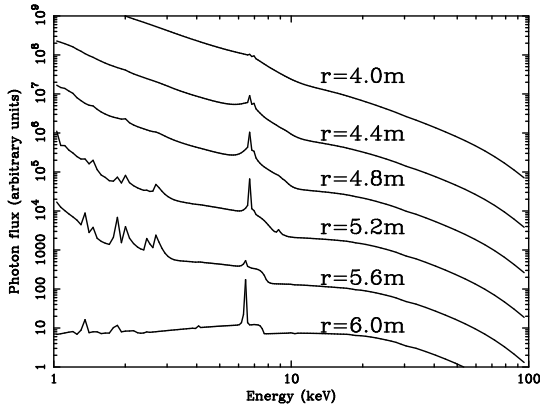


**Figure 2.** Reflected spectra (offset for clarity), computed in a frame in which the gas is at rest, for solar iron abundance. The iron line and absorption edge are clearly seen to vary with radius,  $r$ .

located at a distance  $r = 1000m$  and at an angle  $\theta = 30^\circ$  to the rotation axis of the disc, which is thought to be the inclination angle of the disc in MCG–6–30–15. The accretion disc is assumed to be geometrically thin and located in the plane  $\theta = \pi/2$ , outside the black hole. The accretion flow is divided into two distinct regions, that outside  $6m$  where the particles are assumed to follow Keplerian orbits, and that inside  $6m$  where the particles are assumed to be freely falling into the black hole from the radius of marginal stability. For photon paths that hit the disc we can compute the spectrum that will reach the distant observer from that point. To do this we make use of the fact that the quantity  $I(\nu)/\nu^3$  is invariant along the photon path, where  $I(\nu)$  is the specific intensity at a photon frequency  $\nu$  (Misner et al 1973, p588). We assume that the emission is isotropic, which is a reasonable assumption in this case since the effect of limb darkening is likely to be small as the disc is being viewed almost face on, and the illuminating flux has a high angle of incidence onto the disc (Cunningham 1976). If the point on the disc has an intensity in the rest frame of the accreting matter of  $I(\nu)$  at a frequency  $\nu$ , and in propagating to the observer the photons are redshifted such that a photon emitted at a frequency  $\nu$  is observed at a frequency  $g\nu$ , where  $g = (1+z)^{-1}$  and  $z$  is the redshift, then the flux observed in a frequency interval  $(\nu, \nu + \Delta\nu)$  in a solid angle  $\Delta\Omega$  is then given by

$$F(\nu, \nu + \Delta\nu) = \frac{\Delta\Omega}{4\pi} g^3 I(\nu/g). \quad (1)$$

This takes into account the transformation of the frequency element, and if  $I(\nu)$  is replaced by a delta function at a frequency  $\nu_0$  in the rest frame of the matter we recover the usual  $F \propto g^4 \delta(\nu - g\nu_0)$ .

By integrating over the entire surface of the disc the overall predicted spectrum from the RB97 model may be calculated. We have computed the spectrum in the energy range 1–20 keV where we expect little contribution from photon energies outside the 0.02–100 keV range in which the rest-frame spectra have been calculated. The small direct contribution from the illuminating source itself has also been included.

The spectrum that we predict for the RB97 model is shown in Fig. 3, which appears to consist of a power law

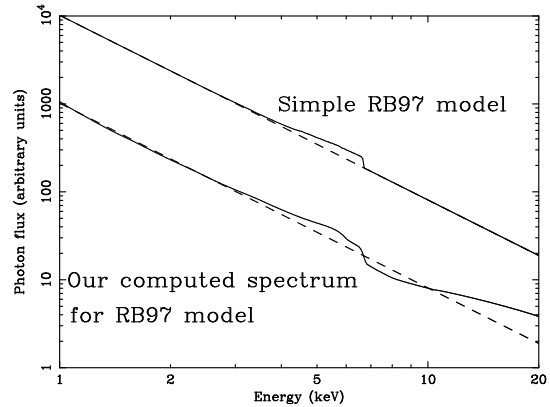


**Figure 3.** A comparison of the spectrum we expect from the RB97 model in which we have computed the reflected continuum in detail in the rest-frame of the matter (lower curve), with a spectrum obtained by adding a power law to the line profile we expect if the reflected continuum in the rest-frame of the matter is approximated by a delta function representing the fluorescent line emission, and the other features of the reflected continuum are ignored (upper curve).

with an extremely broad iron line, an absorption edge, and a Compton reflection component. This particular calculation has been performed for twice solar iron abundance. The precise photon index of the power law component is dependent upon the range of energies over which we fit the predicted spectrum, but is found to be in the range  $\sim 1.9$ – $2.1$ . Fig. 3 also shows the iron line profile computed using the same method as Reynolds & Begelman (1997) in which the iron line is treated as a delta function in the rest-frame of the gas and the other features of the reflected continuum are not considered. Their line profile has been added to a power law for a simpler comparison, and no absorption or Compton reflection components are present. It can also be seen from this figure that the line profile that we predict for their model differs from the profile that Reynolds & Begelman (1997) have calculated.

To obtain a line profile that we can compare with that seen in the data we have fitted our predicted spectrum with a power law between 2–10 keV to obtain the line profile of Fig. 4. For twice solar iron abundance the best fitting power law has a photon index of  $\Gamma = 1.94$ . The iron line profile that we obtain is extremely broad, highly redshifted, and appears to have a bite removed from its high energy end. This bite may be attributed to some of the line flux having fallen into the smeared absorption edge. If we consider the spectrum from the simple RB97 model which approximates the iron line component of the reflected rest-frame spectrum without any of the other features then it does not predict an absorption edge or a bite from the line. In Fig. 4 we have also overlaid the results for solar iron abundance, the effect of which is to reduce the equivalent width of the iron line and the optical depth of the absorption edge.

If we ignore the spectrum outside the range 3–7 keV then the measurable quantities such as the equivalent width of the iron line and the optical depth of the absorption edge are sensitively dependent on the photon index of the power law that is fitted over this energy range. Consider, for example, increasing the photon index of the power law that

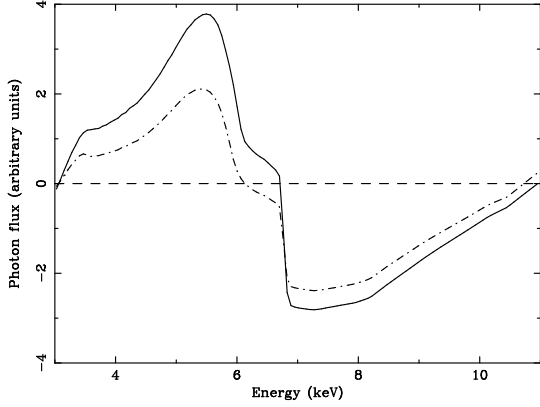


**Figure 4.** Our predicted line profiles for the RB97 model taking into account the full reflected continuum, for both solar (dot-dashed) and twice solar (solid) iron abundance. A best fitting power law has been subtracted from our computed spectrum.

we have fitted to our predicted spectrum of the RB97 model shown in Fig. 3. This would result in the measured equivalent width of the iron line increasing, and the measured optical depth of the absorption edge decreasing. Since the energy range 3–7 keV contains both the broad iron line and the absorption edge the true level of the continuum at a given energy is difficult to estimate, and we would have to consider the spectrum outside this energy range to be able to rule out such a photon index with any certainty. If we now consider Fig. 4, we can see that in fitting a power law to the predicted spectrum between 2–10 keV it is possible for the photon index of the power law to be overestimated, since the deficit of flux above  $\sim 6.5$  keV due to the absorption edge would lead to an underestimate of the true value of the continuum. We may face similar problems when considering the actual X-ray data if we are forced to use a restricted range of energies.

#### 4 MCG–6-30-15

Observations of the Seyfert 1 galaxy MCG–6-30-15 during a deep minimum of its light curve showed the iron line to broaden and extend to lower energies than at other times (Iwasawa et al 1996). This suggested that the source of the iron fluorescence moved inwards so that the observed line had a greater redshift. The best-fitting model for the 0.4–10 keV ASCA SIS spectrum in this interval, using two ionized oxygen absorption edges (Otani et al 1996) and a Laor (1991) line for a maximal Kerr black hole, has a power law with a photon index of  $\Gamma = 1.75^{+0.08}_{-0.03}$ . If we ignore the energy regions with warm absorption and iron emission and just fit the spectrum jointly in the 0.4–0.5, 2.5–3.0 and 7.0–10.0 keV bands then  $\Gamma = 1.71 \pm 0.4$  (reduced  $\chi^2 = 1.2$ ). A similar result is also obtained if we just fit the spectrum in the 2.5–3.0 and 7.0–10.0 keV bands.

In Fig. 5a we have plotted our computed line profile for the RB97 model alongside the X-ray data for the iron line seen in MCG–6-30-15 during the deep minimum of its light curve. To produce our predicted line profile a best fitting power law between 2–10 keV of photon index 1.94 has been subtracted from our predicted spectrum with solar iron

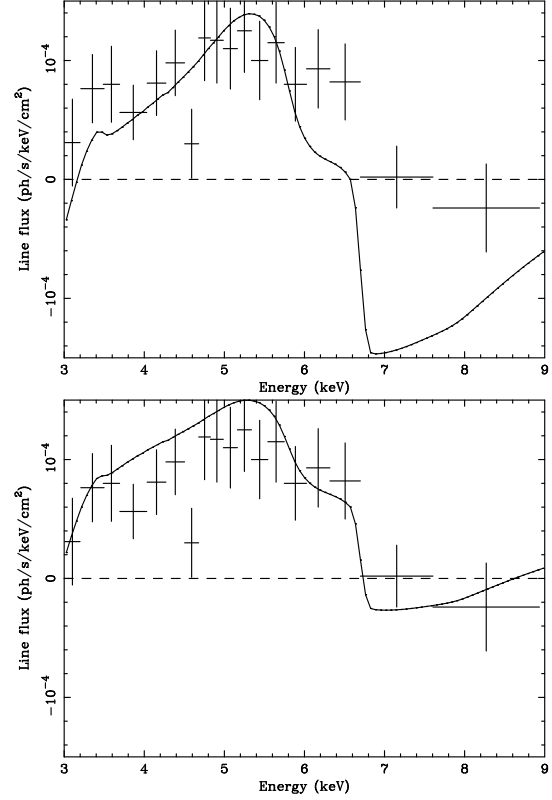


**Figure 5.** Comparisons of our predicted RB97 line profile with the observed data for MCG–6-30-15. In Fig. 5a (upper panel) it is assumed that the underlying power-law index has been accurately measured whereas in Fig. 5b (lower panel) the observed line profile is compared with the pseudo-line created from both the emission and absorption features. This last solution requires an underlying power law have a lower photon index than that observed.

abundance, and to produce the line profile seen in the data a best fitting power law of photon index 1.75 has been subtracted from the data. We see that the predicted line profile possesses a large absorption edge beyond 6.9 keV, which is not present in the data. We therefore conclude that the absence of an iron edge in the data is inconsistent with our calculated spectrum for the physical model of RB97.

In Fig. 5b we show the effect of subtracting a power law with a greater photon index of  $\Gamma = 2.05$  from our predicted spectrum to produce a line profile. As we noted earlier this has the effect of reducing the measured optical depth of the absorption edge. To produce such a fit, however, we would have to assume that the photon index of the power law source decreases even more significantly during the flux minimum of the light curve. This would then cause our computed spectrum to significantly underpredict the flux below the oxygen absorption edges (i.e. below 0.7 keV), by approximately one third. If soft excess emission were used to account for this deficit in flux then it should be detectable in detailed photo-ionization model fits to the warm absorber. Such soft excess emission is not required in fits to the warm absorber in MCG–6-30-15.

## 5 DISCUSSION

We have computed in detail the X-ray spectrum that we would expect to see from the RB97 model for the extremely broad and highly redshifted iron line seen during a deep minimum of the light curve of MCG-6-30-15. Our computation makes use of the full reflected X-ray spectrum including the fluorescent iron line and absorption edge. We predict that the overall observed spectrum should possess an absorption edge, which is inconsistent with the data. We also obtain a different line profile, although with present X-ray telescopes detailed analysis of the shape of the line profile is not possible. It is possible to provide an improved fit to the data but this requires the power law of the X-ray source to have a photon index that is significantly lower than 2. We conclude that the data favour a Kerr over a Schwarzschild black hole model.

Nevertheless, the work of Reynolds & Begelman (1997) has highlighted the potential importance of flows within the marginally stable orbit. If the irradiating X-ray source is at some distance above the disc, particularly in a central location, then fluorescent iron line features from such inflowing material should be observable. That the predicted deep absorption edge is not seen in the case of MCG-6-30-15 supports a Kerr model and, since most of the time the line is not so broad, argues that the irradiating source lies close to the disc and, at times, changes in radius.

The edge in the predicted spectrum of the RB97 model is particularly large because the material is ionized, so enhancing the contrast at the edge. It may be possible to have less highly ionized material within  $6m$  if the accretion disc were gas pressure rather than radiation pressure dominated all the way down to  $6m$  since then the density of the disc would be many times larger. There is also a small edge to the cold disc reflection expected in the standard model. It is unlikely that such a small edge would be detectable with current X-ray telescopes, however.

It is also useful to consider other methods of probing the innermost regions of the accretion disc. If we assume rapid large variations in the continuum are due to flares over the disc, then the time delay between the continuum variation and the fluorescent line response from the disc may be used to estimate the height of the flare above the disc. In the case of the RB97 model this would need to be larger than that for a coronal model in order to provide sufficient illumination of the material within  $6m$ . As well as the time delay between the continuum change and the response of the disc, the evolution of the iron line profile with time can tell us about the geometry of both the source and the disc. Unfortunately with present X-ray telescopes the photon flux in the iron line is only a few hundred counts per day, and integration times are necessarily so large that observations of short term variability are unfeasible.

It is exciting that we are now debating and able to distinguish gross details of the accretion flow of matter at radii less than  $6m$ . Future observations with ASCA, AXAF, XMM, ASTRO-E and Constellation-X will continue this exploration of the very near environment of black holes.

## ACKNOWLEDGEMENTS

AJY and ACF thank PPARC and the Royal Society for support, respectively.

## REFERENCES

- Cunningham C., 1976, *Astrophys. J.*, 208, 534  
 Dabrowski Y. et al., 1997, *Mon. Not. R. astr. Soc.*, 288, L11  
 Iwasawa K. et al., 1996, *Mon. Not. R. astr. Soc.*, 282, 1038  
 Laor A., 1991, *Astrophys. J.*, 376, 90  
 Matt G., Fabian, A.C., Ross, R.R., 1993, *Mon. Not. R. astr. Soc.*, 262, 179  
 Matt G., Perola, G.C., Stellar, L., 1996, *Mon. Not. R. astr. Soc.*, 278, 1111  
 Misner C.W. et al., *Gravitation* (W.H. Freeman and Co., San Francisco)  
 Otani C., 1996, *Publ. astr. Soc. Japan*, 48, 211  
 Rees M.J., Begelman M.C., Blandford R.D., Phinney E.S., 1982, *Nature*, 295, 17  
 Ross R.R., Fabian A.C., 1993, *Mon. Not. R. astr. Soc.*, 261, 74  
 Reynolds C.S., Begelman M.C., 1997, *Astrophys. J.*, 488, 109  
 Tanaka Y. et al., 1995, *Nature*, 375, 659  
 Wilson A.S., Colbert E.J.M., 1995, *Astrophys. J.*, 438, 62